Renewable Energy 66 (2014) 662–669

Contents lists available at ScienceDirect

Renewable Energy

journal homepage: www.elsevier.com/locate/renene

Technical note

Numerical and experimental assessment of a downdraft gasifier for electric power in Amazon using açaí seed (*Euterpe oleracea* Mart.) as a fuel

Yuu Itai [a], Robson Santos [a], Mónica Branquinho [b], Isabel Malico [b,c], Grace F. Ghesti [d,*], Augusto M. Brasil [e]

[a] Universidade Federal do Pará, Faculdade de Engenharia Mecânica, Rua Augusto Correa, 01, 66075-900 Belém, PA, Brazil
[b] Physics Department, University of Évora, R. Romão Ramalho, 59, 7000-671 Évora, Portugal
[c] IDMEC/IST, University of Lisbon, Mechanical Engineering Department, Av. Rovisco Pais, 1049-001 Lisbon, Portugal
[d] Universidade de Brasília, Campus Darcy Ribeiro, Instituto de Química, Caixa Postal 4478, Brasília, 70904-970 DF, Brazil
[e] Universidade de Brasília, Faculdade UnB Gama, Área especial de indústria projeção A – UnB Setor leste Gama, 72444-240 DF, Brazil

ARTICLE INFO

Article history:
Received 29 January 2013
Accepted 8 January 2014
Available online 11 February 2014

Keywords:
Residual biomass
Isolated communities
Power production
Downdraft gasifier
Thermal equilibrium modeling
Experiments

ABSTRACT

The Amazon region is characterized by communities isolated from the grid that currently are using diesel engines to produce electricity and that have residual biomass energy potentials between 60 and 500 kW. In this scenario, gasification appears as an evident choice as far as energy generation is concerned. Other than wood, açaí seed is the biomass residue most wasted in the Pará State and its use in gasification systems is assessed in this study. With this purpose, a cylindrical bodied downdraft gasifier was designed, built and tested, and an equilibrium model implemented. The comparison of the simulation values with the experimental and numerical results of other authors show that they are in-line with the predictions of other equilibrium models. Also, they confirm that this kind of models is a fast and useful tool for a preliminary assessment of the applicability of a specific biomass gasification process for electricity production. Moreover, the deviation between the numerical and experimental results obtained in this study was lower around the equivalence ratio that optimizes the gasification process (in the 2.15–2.3 range). As far as biomass humidity is concerned, the producer gas calorific value and cold gas efficiency decrease with an increase in this parameter.

1. Introduction

Pará is a Brazilian federal State located in the Amazon basin (circled in Fig. 1). The 2011 Brazilian Energy Balance shows that the amount of electricity generation of the entire northern region of Brazil is 63,152 GWh, and that the Pará State shares 63.3% of that generation. However, the electricity residential consumption of the State is only 2406 GWh. Simultaneously, the diesel generators installed power in Pará is 153.5 MW resulting in a consumption of almost 250 million liters annually.

The electric grid is managed by ELETROBRAS, a company controlled by the Brazilian Government. According to ELETROBRAS there are 1.2 million consumers in the Amazon region that are not connected to the grid [2]. Thermal power plants in Brazil are scattered as shown in Fig. 1a and biomass power plants are shown in Fig. 1b. Those two figures confirm that in Amazon region, as well as in Pará State, virtually all thermal power plants are diesel fueled (natural gas and coal are not used).

As showed above, the Amazonian scenario is dominated by communities isolated from the electric grid using diesel to generate electricity, yet the Amazon region provides good climate and biomass availability that can be used as renewable energy source for isolated communities. Padilha [3] assessed the residual biomass energy potential in Pará State indicating that 43% of the villages would allow for an installed capacity of 200 kW and 81% would between 60 kW and 500 kW (Fig. 2). With such low electric potential up to 300 kW, power plants with combustion and steam turbines have less applicability when compared to gasification systems due to the overall efficiency.

Fig. 3 presents jointly the data published by Bridgewater [4], Dornburg and Faaij [5] and Caputo et al. [6]. Those authors showed that for smaller power plants gasification systems have higher efficiencies than combustion systems with steam cycle. Having this in

* Corresponding author. Tel.: +55 6192772610.
E-mail addresses: imbm@uevora.pt (I. Malico), grace@unb.br (G.F. Ghesti), ambrasil@unb.br (A.M. Brasil).

0960-1481/$ – see front matter © 2014 Elsevier Ltd. All rights reserved.
http://dx.doi.org/10.1016/j.renene.2014.01.007

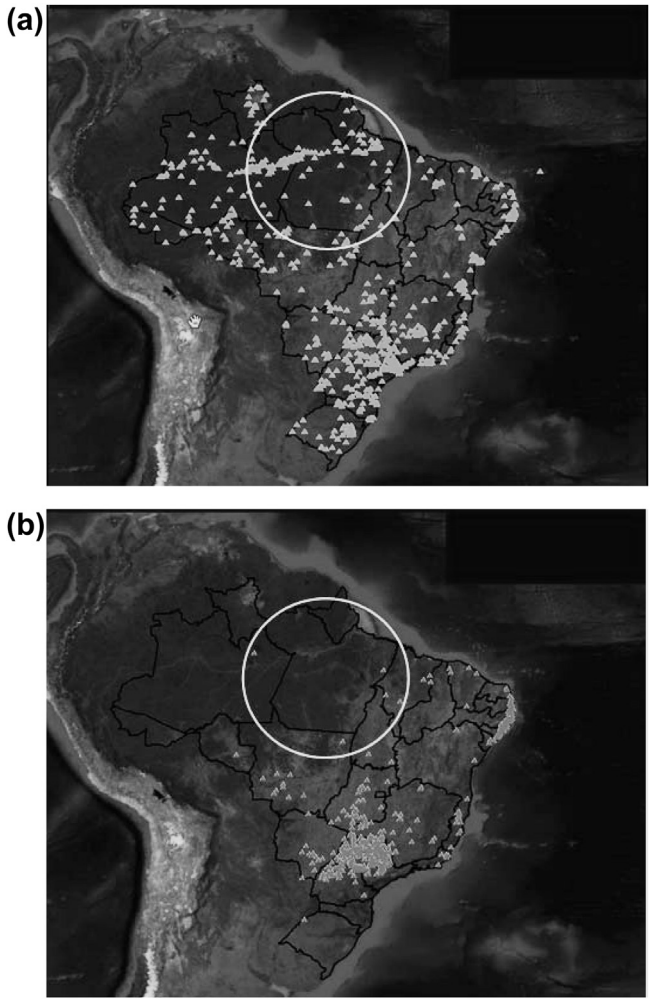

Fig. 1. (a) Thermal power plants in Brazil; (b) Biomass fueled power plants in Brazil. The State of Pará is the one enclosed in the white circle. Source: ANEEL [1].

mind, gasification systems are very suitable to the needs of Amazonian communities: one because of the availability of biomass in the region, and two because of the higher efficiency compared to the systems using combustion and steam turbines. Diesel engines are already in operation in the Amazon region producing electric energy (as long as the small communities are not

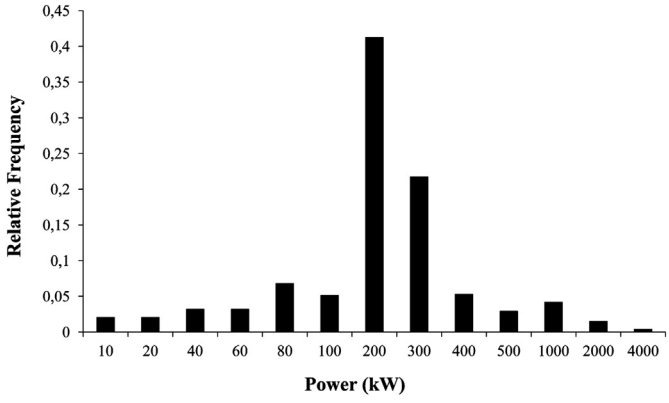

Fig. 2. Histogram of the residual biomass electric potential for State of Pará [3].

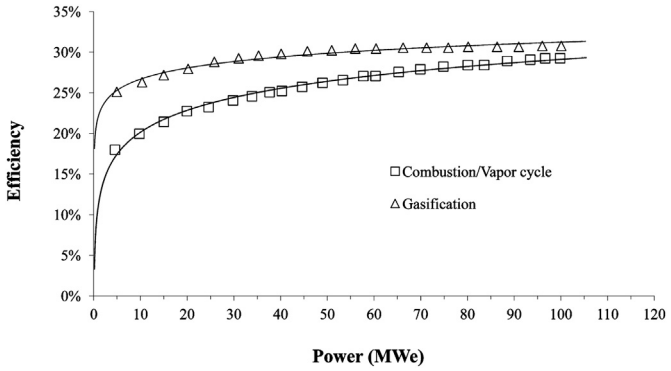

Fig. 3. Power plant efficiency as a function of the delivered electrical power. Adapted from Refs. [4–6].

connected to the grid), and gasification systems would fit the actual infrastructure. However, the potential of biomass as energy source for small Amazonian communities can only be evaluated through optimized operation and design of gasifier reactors together with simulation models that can predict the gasification efficiency and the producer gas heating value.

Apart from woody biomass residues, açaí seed (*Euterpe oleracea* Mart.) is the biomass residues most wasted in Pará State (Brazil) due to a production of 106 kton/year of that fruit. However, wastes of açaí seeds can be up to 70% moist and that could make the gasification process unviable. Again, optimization of the gasifier design, operating parameters and numerical simulations can overcome problems caused by moisture content concerning the gasification process of açaí seeds.

Therefore, when using açaí seeds as an energy source in gasification systems for isolated communities, best compositions of producer gas are achieved when three conditions are observed: first the design of the reactor, second the operating parameters of the gasifier, and third the influence of the feedstock properties such as geometry, moisture content and elemental composition.

From the design point of view, as showed in Fig. 2, isolated communities in the State of Pará can only generate an average 200 kW of electric power. As a result, for such small-scale systems, fixed bed downdraft gasifiers are the simplest and most applicable design [7–9].

In terms of the gasifier operation, air/fuel ratio and humidity are the parameters that highly influence the producer gas composition and gasification efficiency.

As feedstock properties, açaí seed holds a good geometry being almost a sphere with average diameter of 10 mm [10]. Yet, wasted açaí seeds can be up to 70% moist and can be kept with moisture content not lower than 10% when disposed in open environment. Those characteristics and elemental analysis of açaí seeds shown ahead in item 2 indicate good potential for gasification instead of combustion.

Previous studies preformed by other authors determined if certain residues relevant in a specific region are suitable for gasification. For example Ref. [11], presents an experimental study on the gasification of pine wood, eucalyptus wood, rice husk and nut shell. They showed that these residues are suitable for energy production using gasification. In another study [12], almond residues (almond shell, almond pruning and almond shell peel) were studied in a laboratory fixed bed gasifier by the some group. In Ref. [13], a biomass gasifier was installed in a small community in South Africa. The study establishes that the residues obtained in a sawmill meet the requirements for the gasifier considered and that the running of the gasification unit has a considerable impact on the

community. Also giving attention to the application of biomass gasification as an energy resource the work of Ref. [14] studied experimentally the gasification of rice husk and rice husk pellets and showed the possibility of stable power generation using synthetic gas from residues obtained from rice mills. Whereas Ref. [15], focuses on agriculture residues (corn stalks, sunflower stalks and rapeseed straw) and their use in a downdraft gasifier. These residues are compared by means of the results obtained with a chemical equilibrium model. Ref. [16] focused on olive oil industry wastes and modeled a small-scale plant based on a downdraft gasifier and a gas engine, obtaining high gasification efficiencies.

With the evidences pointing to the adequacy of simple designed gasifier and fine feedstock properties, the question resides if açaí seed is applicable in downdraft gasification systems for electric power generation, resulting in good quality producer gas. The question can be answered allying a numerical and experimental study, as done in this work. The main objective of this work is to study the gasification of the açaí seed and evaluate the influence of the main operating conditions and biomass characteristics on the producer gas composition and efficiency of the process.

2. Material and method

2.1. Gasifier and biomass characterization

An experimental cylindrical bodied downdraft gasifier was developed for the present work to analyze gasification reactions of açaí seeds in a fixed bed. Some authors [7–9] refer to simple design and fixed bed downdraft gasifiers being more indicated for small-scale systems. Downdraft type and cylindrical design are also justified by the fact that, for up to 200 kW and internal combustion engine applications, downdraft gasifiers are more suitable than updraft since they provide relatively tar free and clean gases [17].

Fig. 4 shows the schematic of the gasifier and equipment used for the experimental evaluation.

Components of the experimental set-up consisted of an air inlet tube with flow measurement system, a cylindrical bodied stratified downdraft reactor, a gas sampling train and a producer gas outlet connected to an exhauster blower.

The air inlet at the top of the gasifier was composed of a PVC tube with 52 mm of inner diameter and 1230 mm long with a flow control valve. A Pitot tube was installed in the inlet tube, 520 mm away from the from tube entry at the fully developed region, and connected to a flow meter.

The downdraft gasifier comprised a ceramic inner core cylindrical reactor, thermal insulation layer and steel case. Inner cylindrical reactor ((e) in Fig. 4) made of refractory tube material circa 50% Al_2O_3 and 50% SiO_2 having 150 mm of inner diameter and 50 mm of thickness. Thermal insulation was achieved by a blanket fiber layer between the ceramic reactor and steel case. Insulation blanket was 45–47% Al_2O_3 and 45–47% SiO_2 with 160 kg/m^3 of density. Holes with 2 mm were equally bored longitudinally spaced 10 mm from each other so thermocouples could be inserted in the biomass bed ((d) in Fig. 4).

A bottom section contained a grate 1500 mm distant from the top of the reactor. The grate could move sideward as a drawer in order to open entirely the bottom of the reactor for cleaning. The section immediately below the grate served as an ashbin made with the same material of the steel case. An exhaust pipe with 52.5 mm of inner diameter, attached to the reactor steel case below the grate level, served as the producer gas outlet where the gas sampling probe was positioned.

All experimental values were stored in a PC with a data logger acquisition system (CONTEMP A202) integrating analog and digital signals with 1 Hz of acquisition rate.

Air inlet flow was measured using the Pitot tube connected to a micromanometer (FCO510 FURNESS CONTROLS) and a thermocouple type K ((a) in Fig. 4). The micromanometer had an RS232 port connected to the PC data logger so the data of the differential pressure measured by the Pitot and temperature were used to calculate air inlet flow.

Producer gas outlet flow ((f) in Fig. 4) was measured similarly to the air inlet flow, but a Venturi was used instead of Pitot tube to avoid tar condensation blocking the Pitot. Differential pressure data

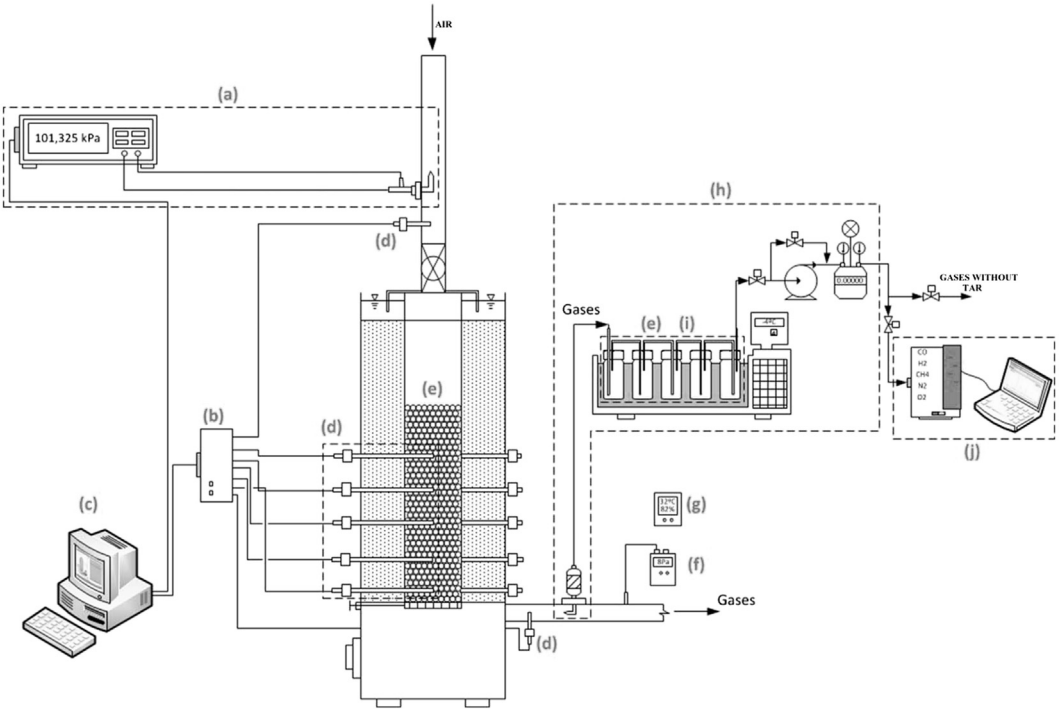

Fig. 4. Schematic of the gasifier and equipment used for the data acquisition.

of the Venturi were also acquired by the micromanometer, and together with the temperature of the outlet producer gas the flow was calculated.

Temperatures of the air inlet, outlet producer gas and biomass bed were measured using thermocouples type K ((d) in Fig. 4) with ±8 °C of accuracy in the range of 800–1200 °C. Thermocouples were connected to an acquisition board with cold junction compensator with sampling rate of 1 Hz, and that board was also connected to the PC data logger.

Producer gas samples were taken at the bottom of the gasifier. Firstly the gas samples passed through a heated glass fiber filter maintained within a temperature range of 300–350 °C for the particle capture. There was a moisture and tar collector train before sending the gas sample to a Micro-Gas Chromatograph (VARIAN CP-4900). The collector train consisted of five impinger bottles immersed in ice bath. Each of the five impinger bottles contained 100 ml of isopropanol. A vacuum pump with capacity of 127 l/min (ACTARIS) was used to accurately measure the gas sample flow. For the ice bath a cooling mixture of salt, ice and water was used.

Producer gas composition was measured by the Micro-Gas Chromatograph VARIAN CP-4900 with samples taken periodically from the outlet producer gas. Volume fractions of H_2, CO, CH_4 and CO_2 were determined.

Table 1 presents the ultimate and proximate analyses of the açaí seed. A PerkinElmer 2400 CHN was used for the açaí seed ultimate analysis, and the higher heating value of biomass in dry basis, HHV_{db}, was measured using a calorimeter IKE WERKE C2000. Latter the lower heating value was determined from the HHV_{db} and from the hydrogen content.

2.2. Mathematical model

A recent review on biomass gasification models can be found in Ref. [18]. The most simple are the equilibrium models that only consider the composition of the final products. Examples of the application of this kind of models to the simulation of downdraft gasifiers can be found, for example, in Refs. [15,17,19–23]. Non-equilibrium models, which consider the different processes that occur along the gasifier, were also developed for the simulation of downdraft gasifiers (see for example, Refs. [24–28]). These models describe the char reduction process using chemical kinetics, are accurate and essential when the residence time of the reactants is relatively short. However, they are computationally intensive and dependent of the gasifier design.

In downdraft gasifiers, equilibrium is established after a relatively short period of time, since both pyrolysis and gasification products pass through the hottest zone of the equipment [17]; this fact supports the use of equilibrium models. Furthermore, several authors [19,29] confirmed the validity of this kind of models for fixed-bed downdraft gasifiers.

Table 1
Proximate and ultimate analysis of the açaí seed.

Proximate analysis	
Ashes (%, db)	1.39
Volatiles (%, db)	79.93
Carbon fixed (%, db)	18.68
Moisture content (%, db)	15.48
Ultimate analysis	
C (%, db)	46.04
H (%, db)	6.77
O[a] (%, db)	38.38
N (%, db)	7.99
S (%, db)	0.08
Higher heating value (kJ/kg)	18,141

[a] Sum of oxygen with other species (O = 44.22, Cl = 0.21, $F \leq 0.20$ and $P = 0.067$).

Zero dimensional equilibrium models slightly differ from each other in terms of the premises and the gasification reactions involved. Their predicted composition of the producer gas not always gives highly accurate results, but they are a useful tool for preliminary comparison [29]. For this reason, several attempts of modifications have been proposed such as the correction of the equilibrium constants or the quasi-equilibrium approach (e.g., Refs. [29–31]). Still, zero dimensional pure equilibrium models are fast to run and do not demand powerful computers. Therefore, such light models are very useful to infer the influence of the gasifier design and operational parameters on the producer gas species concentration, so those models are applicable to estimate the chemical reactions occurring in gasification of Amazonian biomass with high moisture content and assessing if they can be used as a renewable energy source for isolated communities in Amazon.

The implemented model comprises the energy conservation equation, species atomic mass conservation equations and Gibbs free energy minimization equations. It assumes that all products leaving the gasifier are low molar mass gases, namely CO_2, CO, H_2, H_2O, CH_4, N_2 and SO_2. Note that downdraft gasifiers usually operate with high carbon conversion and result in a low tar content gas [18]. Therefore, it was assumed that all carbon was converted in the gasifier. The next sections describe the model used in the present work.

2.2.1. Biomass

The coefficients of the biomass representative formula, $C_{c1}H_{c2}O_{c3}N_{c4}S_{c5}$, are determined from the ultimate analysis as:

$$c_i = \frac{y_{i,d}}{y_{1,d}}\frac{M_1}{M_i} \quad i = 1, 2, 3, 4 \text{ and } 5 \tag{1}$$

where M_i and $y_{i,d}$ are, respectively, the molar mass and mass fraction on a dry basis of the ith species. Note that c_1 is equal to 1.

The representative molar mass of the biomass, M_b, is given by the components in its formula, as:

$$M_b = \sum_{i=1}^{5} c_i M_i \tag{2}$$

The molar quantity of water per mole of the biomass, α, is related to its relative humidity, h, by:

$$\alpha = \frac{M_b h}{M_{H_2O}(1-h)} \tag{3}$$

The representative formation enthalpy of the biomass, $\overline{h}_{f,b}$, is determined from the higher heating value of the biomass in dry basis, $HHV_{b,d}$, obtained experimentally:

$$\overline{h}_{f,b} = HHV_{b,d} M_b + \sum_{i=\text{Prod}} \nu_i \overline{h}_{f,i} \tag{4}$$

where ν_i are the stoichiometry coefficients of the products on the biomass stoichiometry reaction and $\overline{h}_{f,i}$ their formation enthalpy.

2.2.2. Chemical and thermodynamic equilibrium

The global reaction in the downdraft gasifier can be written as

$$CH_{c_2}O_{c_3}N_{c_4}S_{c_5} + \alpha H_2O + \beta(O_2 + 3.76N_2) \rightarrow a_1CO_2 + a_2CO + a_3H_2 + a_4H_2O + a_5CH_4 + a_6N_2 + a_7SO_2 \tag{5}$$

As already stated, it was assumed that chemical equilibrium is achieved and that, in downdraft gasifiers, the content of tars and

char in the final gas can be neglected. It was also assumed that no oxygen is present in the producer gas, based on the fact that, typically, during the gasifying process the equivalence ratio is high (a typical equivalence ratio for a gasification process is 4 [7]).

The variable β is related to the equivalence ratio, Φ, by:

$$\Phi = \frac{(A/F)_s}{A/F} = \frac{\beta_s}{\beta} \tag{6}$$

where A/F is the air–fuel ratio and s stands for the stoichiometric reaction.

The atomic mass species conservation equations result in:

$$1 = a_1 + a_2 + a_5 \tag{7}$$

$$c_2 + 2\alpha = 2a_3 + 2a_4 + 4a_5 \tag{8}$$

$$c_3 + \alpha + 2\beta = 2a_1 + a_2 + a_4 + 2a_7 \tag{9}$$

$$c_4 + 7.52\beta = 2a_6 \tag{10}$$

$$c_5 = a_7 \tag{11}$$

To be able to solve the above equations, two equilibrium reactions have to be considered.

The water gas shift reaction describes the equilibrium between CO and H_2 in the presence of water.

$$CO + H_2O \leftrightarrow CO_2 + H_2 \tag{12}$$

The equilibrium constant as a function of the molar composition, assuming the producer gas as an ideal gas and that the pressure of the gasifier is 1 atm, reads:

$$K_1 = \frac{a_1 a_3}{a_2 a_4} \tag{13}$$

In the reduction zone of the gasifier, hydrogen is reduced to methane by the carbon.

$$C + 2H_2 \leftrightarrow CH_4 \tag{14}$$

The equilibrium constant as a function of the molar composition, assuming the producer gas as an ideal gas and that the pressure of the gasifier is 1 atm, reads:

$$K_2 = \frac{a_5 n_t}{a_3^2} \tag{15}$$

where n_t is the total number of moles of the producer gas for 1 mol of dry biomass.

The values of the equilibrium constants are calculated by minimizing the Gibbs free energy as

$$K_1 = \exp\left(-\left(\bar{g}^0_{T,H_2} + \bar{g}^0_{T,CO_2} - \bar{g}^0_{T,CO} - \bar{g}^0_{T,H_2O}\right)\Big/RT\right) \tag{16}$$

$$K_2 = \exp\left(-\left(\bar{g}^0_{T,CH_4} - 2\bar{g}^0_{T,H_2}\right)\Big/RT\right) \tag{17}$$

with

$$\bar{g}^0_{T,i} = \bar{h}_i - T\bar{s}^0_i \tag{18}$$

where $\bar{g}^0_{T,i}$, $\bar{h}_i$ and s^0_i are, respectively, the Gibbs free energy, the absolute enthalpy and the entropy of the ith species at temperature T. Their values are obtained from Ref. [32].

The steady-state integral energy conservation equation is used to determine the producer gas temperature, T_p. Since the work produced during the gasification process is zero and the heat losses are small, this equation reads:

$$\sum_{Reac} \nu_i \left(\bar{h}^0_{f,298} + \int_{298}^{T_R} \bar{c}_p dT\right)_i = \sum_{Prod} \nu_i \left(\bar{h}^0_{f,298} + \int_{298}^{T_P} \bar{c}_p dT\right)_i \tag{19}$$

where ν_i are the stoichiometry coefficients of the global gasification reaction and $\bar{h}^0_{f,298}$ and $\bar{c}_p$ the formation enthalpy at 298 K and the specific heat, respectively. The formation enthalpy and the specific heats were obtained from Ref. [32].

2.3. Numerical model

Eqs. (7)–(11), (13), (15) and (19) define a system of eight non-linear equations that can be solved to determine the seven a_i coefficients and the temperature of the producer gas. The algorithm used to solve these equations is the following:

1. An initial guess for the producer gas temperature, T_p, is made.
2. The producer gas composition is calculated from Eqs. (7)–(11), (13) and (15) for T_p.
3. A new value for T_p is calculated from Eq. (19).
4. Steps 2 and 3 are repeated until chemical and thermodynamic equilibrium is reached.

The non-linear system of equations used to obtain the producer gas composition (Eqs. (7)–(11), (13) and (15)) were solved by the Newton–Raphson method to solve non-linear systems of equations. Also, the energy equation (Eq. (19)) was solved using the Newton–Raphson method.

3. Results and discussion

3.1. Model validation

The results obtained with the model implemented in this paper have been compared to the experimental and numerical results of other authors. The first comparison was based on the producer gas composition presented by Jayah et al. [26]. These authors conducted experimental testing on an 80 kW_{th} downdraft gasifier fueled with rubber wood (*Hevea brasiliensis*). The details of the experimental setup can be found in Ref. [26] and the experimental results in Table 2. Jayah et al. [26] also present numerical predictions obtained with a 1D model. These results were calibrated by the methane content and are shown in Table 2. The predictions of Melgar et al. [21] and Rodrigues [33] are also presented in Table 2, along with the predictions obtained with the model described in this paper. For the present calculations, the equivalence ratio used was the one calculated by Melgar et al. [21], 2.39. It can be seen that

Table 2
Comparison between experimental results and prediction for the producer gas of rubber wood.

Producer gas composition (vol%)	CO_2	CO	H_2	CH_4	N_2
Experimental data [26]	11.4	19.1	15.5	1.1	52.9
1D predictions [26]	11.1	18.3	16.4	1.1[a]	53.2
0D predictions [21]	11.1	19.3	17.6	0.4	51.6
0D predictions [33]	11.6	19.3	20.7	0.9	47.5
Present work	11.9	18.2	17.7	0.6	51.6

[a] Assumed.

all the three 0D models have the same level of accuracy, which is considered good. The 1D model of Jayah et al. [26], with a maximum difference of 5.8% between predictions and experiments, shows better accuracy than the 0D models considered in Table 2. However, it should be noticed that the 1D numerical results were calibrated by the experimental methane content. In fact, the biggest difference between the present model and the experimental data is in the methane fraction of the producer gas. None of the 0D models considered heat losses in the gasifier, which in reality did not have any insulation. This justifies in part the difference in the predicted methane and hydrogen contents. But only in part, since intrinsic reasons due to the simplifications imposed by the equilibrium model also exist. In fact, the model assumes that there are no tars and no char in the producer gas and that chemical equilibrium is reached. Equilibrium in reality never takes place in a gasification process, particularly at temperatures below 800 °C [20]. All the equilibrium 0D models analyzed overestimate the hydrogen production and underestimate the methane production, since in reality no chemical equilibrium is reached, especially for the methane reaction. Since the predicted methane content is lower, and carbon is only present in the producer gas in the form of CH_4, CO and CO_2, an underestimation of CH_4 leads to an overestimation of the CO and CO_2 contents (an exception is the carbon dioxide content obtained by Melgar et al. [21] that is underestimated).

The second validation case considered in this paper was the comparison between the results obtained with the present 0D model and the one used in Tinaut et al. [34]. The biomass used in the simulations was pine bark and several moisture contents (10, 20 and 30%) and equivalence ratios (3 and 4) were considered. Table 3 presents the producer gas composition presented in Tinaut et al. [34] and the predicted with the current model.

The present results are in line with the obtained by Tinaut et al. [34]. Since these authors used a similar thermal equilibrium model to the one presented in this paper, this gives confidence to the present results. The biggest differences, 4%, were obtained for the methane content when the operating conditions are: 20% biomass humidity content and equivalence ratio equal to 3.

3.2. Açaí gasification

After comparing the results obtained with the present model with experimental results and predictions of other authors, the simulation of the gasification of açaí seeds under several operating conditions was undertaken. Both experimental and numerical results will be presented in this section and compared. The açaí seeds ultimate analysis was already given in Table 1 and the considered reactants temperature is 304.95 K. The equivalence ratio was varied between 1.5 and 4.0 in the simulations and between 1.63 and 3.14 in the experiments.

Fig. 5 shows the comparison between the measured and predicted producer gas composition on a dry basis. It can be seen that the hydrogen content increases with an increase in the equivalence ratio until a maximum and then decreases. The peak is obtained for $\Phi = 2.14$ in the experiments, while in the simulations for $\Phi = 2.6$. This is in-line with the predictions of, for example, Refs. [21,28]. It should be mentioned that other authors (e.g., Refs. [17,29]) do not predict this maximum in the hydrogen composition and report a continuous increase in the hydrogen production with the equivalent ratio. This can be explained by the fact that they analyzed different gasification conditions (a shorter equivalence ratio range, for example). Moreover, Fig. 5 shows that the thermal equilibrium model overestimates the hydrogen production for this equivalence ratio range (the same generally happens with the predictions of, for example, Refs. [21,29,33]). The fact that the model does not account for thermal losses, explains partially this overprediction. If we consider heat losses, the numerical results generally get closer to the experimental. Table 4 shows the comparison between experimental and numerical results obtained considering variable heat losses. With a trial and error procedure, the percentage of heat losses in relation to the biomass energy input was varied until the predicted methane or carbon monoxide contents were equal to the experimental values. For most cases, methane is the gas that shows bigger differences between simulations and experiments, so, similarly to Jayah et al. [26], the results were calibrated for the methane content. However, for the higher equivalence ratios, increasing heat losses would increase the difference between experimental and simulated methane content, so, in this cases, the results were calibrated for carbon monoxide. In Table 4, the chemical specie that was used for this tuning is indicated in bold (For the lower equivalence ratios it was methane and, after $\Phi = 2.33$, carbon monoxide). Note that, in general, the calculated heat loss is higher when the equivalence ratio is lower, which is consistent with the fact that in this case the temperatures are higher, and therefore more heat losses exist.

It can be seen from Table 4 that, when heat losses are considered, the hydrogen volume fraction predictions get slightly closer to the experimental values ($\Phi = 1.63$ is an exception). However, the predictions are still consistently higher than the experiments.

Fig. 5 also shows the comparison between the measured and predicted methane volume fraction of the producer gas on a dry basis. It can be seen that the thermal equilibrium model overestimates the methane production for high equivalence ratios and underestimates it for low equivalence ratios. For example, Melgar et al. [21] also show the same trend. For low equivalence ratios, the

Table 3
Comparison between the prediction of the present model and the results of Tinaut et al. [34] for the producer gas of pine bark.

Producer gas composition (vol%)	CO_2	CO	H_2	CH_4	N_2	h	Φ
Tinaut et al. [34]	9.4	24.3	18.0	1.8	46.5	0.1	3
Present work	9.5	24.2	17.9	1.8	46.5	0.1	3
Tinaut et al. [34]	13.0	19.5	19.2	2.5	45.8	0.2	3
Present work	13.1	19.3	19.1	2.6	45.9	0.2	3
Tinaut et al. [34]	17.0	14.2	19.9	3.6	45.4	0.3	3
Present work	17.1	14.0	19.8	3.6	45.5	0.3	3
Tinaut et al. [34]	11.2	24.9	15.8	6.4	41.7	0.1	4
Present work	11.3	24.7	15.7	6.6	41.8	0.1	4
Tinaut et al. [34]	16.2	18.0	17.4	7.4	40.9	0.2	4
Present work	16.4	17.8	17.3	7.5	41.0	0.2	4
Tinaut et al. [34]	21.2	11.3	18.1	8.8	40.6	0.3	4
Present work	21.4	11.1	17.9	8.9	40.7	0.3	4

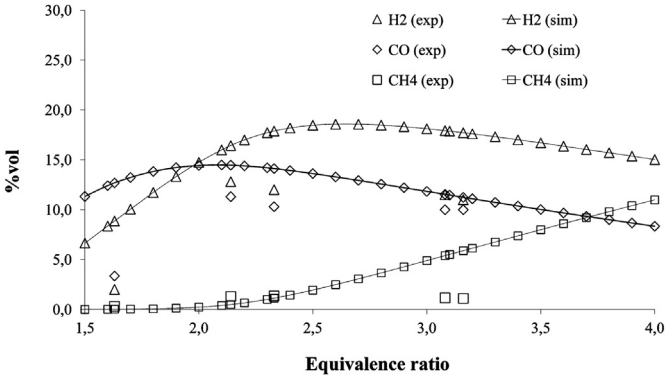

Fig. 5. Measured (exp) and predicted (sim) producer gas composition on a dry basis for the açaí seed gasification.

Table 4
Experimental and predicted producer gas composition considering heat losses in the gasifier.

Producer gas composition (vol%)	CO	H_2	CH_4	N_2	Φ
Experimental results	3.34	2.00	0.31	60.48	1.63
Predictions (17% heat loss)	8.80	11.16	**0.31**	64.71	1.63
Experimental results	11.30	12.80	1.30	55.87	2.14
Predictions (6% heat loss)	11.69	16.13	**1.30**	56.39	2.14
Experimental results	10.30	12.00	1.35	55.23	2.33
Predictions (1% heat loss)	13.48	17.71	**1.35**	53.83	2.33
Experimental results	10.00	11.50	1.16	56.35	3.08
Predictions (2% heat loss)	**10.00**	16.73	6.23	49.26	3.08
Experimental results	10.00	11.00	1.10	56.20	3.16
Predictions (2% heat loss)	**10.00**	16.70	6.60	48.79	3.16

underprediction can be partially explained by the fact that no heat losses were accounted in the numerical model. When heat losses were included in the model, the methane content got closer to the experiments for the low equivalence ratios (see Table 4). However, for the higher equivalence ratios, considering heat losses only increases more the predicted methane content, which is already overestimated. The experimental results show that there is a peak of methane production for $\Phi = 2.33$, while the simulations show that the methane content increases continuously with the equivalence ratio. The different behavior of the experimental and overpredicted methane volume fraction curves at higher equivalence ratios is explained by the fact that chemical equilibrium is not achieved in the real gasification process and that not all the carbon is converted.

Fig. 5 also shows the comparison between the measured and predicted carbon monoxide volume fraction of the producer gas on a dry basis. Similarly to the hydrogen content, the CO volume fraction has a peak for a specific equivalence ratio. Both for the experiments and simulations, this maximum CO content was obtained for and equivalence ratio of around 2.1. Similarly to hydrogen, this peak was predicted, for example by Refs. [21,28], but not by other authors (e.g., Refs. [17,29]). This difference can be explained in the same manner. From Fig. 5, it can be seen that the thermal equilibrium model overestimates the carbon monoxide production, especially for the lower equivalence ratios. Looking at Table 4, one can see that, if heat losses are considered, the predictions are close to the experimental values (again, $\Phi = 1.63$ is an exception).

Fig. 6 presents the comparison between measured and predicted gasification temperature as a function of the equivalence ratio. As the equivalence ratio approaches unity, the reaction moves towards stoichiometric combustion and thus the temperature should increase, as predicted by the model (line in Fig. 6). However, although the experimental results follow this trend, they do not show a big variation of the temperature with the equivalence ratio. This is a clear indication that heat losses existed during the experiments. For equivalence ratios less than 2.33, the simulated adiabatic temperature values diverge from the experimental temperature values. However, for the same range of equivalence ratios, if heat losses are considered in the model, simulated values agree with measured temperature values. Differently, for equivalence ratios higher than 2.33, both simulated temperature values (with or without heat losses) agree and diverge from experimental values. Gasification temperature results indicate that only when equivalence ratios are less than 2.33 do the heat losses explain why simulated temperatures do not agree with measured temperature values. That indicates the lower is the equivalence ratio the higher is the energy produced by chemical reactions resulting in more heat losses. On the other hand, the higher the equivalence ratio the lower is the energy by chemical reactions because the greatest part of the energy is carried by the producer gas.

CO, CH_4 and H_2 are the relevant producer gases, since the others do not significance as far as energy conversion is concerned. If one looks at the experimental results, and for 15.48% biomass humidity, the equivalence ratios that lead to higher cold gas efficiency and heating values of the producer gas are 2.14 and 2.33, respectively. Simulation results indicate that heat loss does not influence much the cold gas efficiency, therefore only the efficiency results where no heat loss were considered are presented. Equivalence ratios lower than 2.33 should result in lower cold gas efficiency predictions, as in the case of the experimental values in Fig. 7, because when the equivalence ratio tends to 1 only CO_2 and H_2O are expected in the produce gas. For equivalence ratios greater than 2.33, char formation during the real gasification process can explain the decrease in the experimental values of the cold gas efficiency (and also explains the overestimation of the simulated CH_4 content). Erlich and Fransson [35], who performed an experimental study on a downdraft gasifier, also report an increase of the cold gas efficiency with a decrease in the equivalence ratio and state that the efficiency has an upper limit since then the process approaches combustion.

If only the prediction results were analyzed, due to the methane content overestimation, one would conclude that the higher equivalent ratio the better (Fig. 7). However, as already explained, this is not the case. According to Desrosiers [36], apud Puig-Arnavat et al. [29], and Double and Bridgewater [37], apud Puig-Arnavat et al. [29], the carbon boundary point, CBP, is the optimum point for gasification as far as energy-based efficiency is concerned and takes place when exactly enough air is added to avoid carbon formation. This means that, according to the present experiments, the

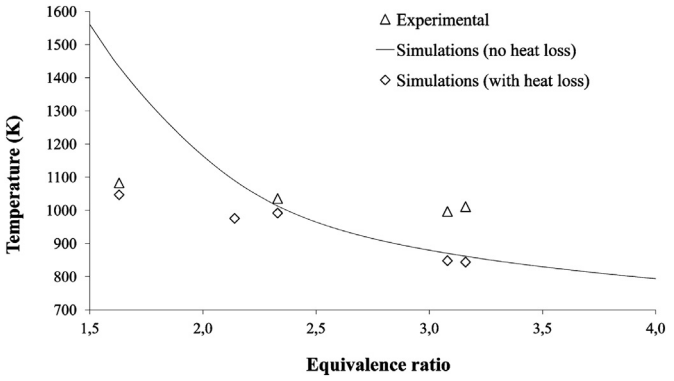

Fig. 6. Measured and predicted gasification temperature.

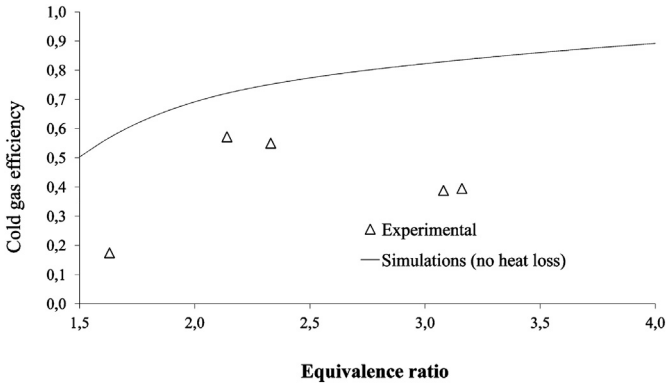

Fig. 7. Measured and predicted cold gas efficiencies for the açaí seed gasification.

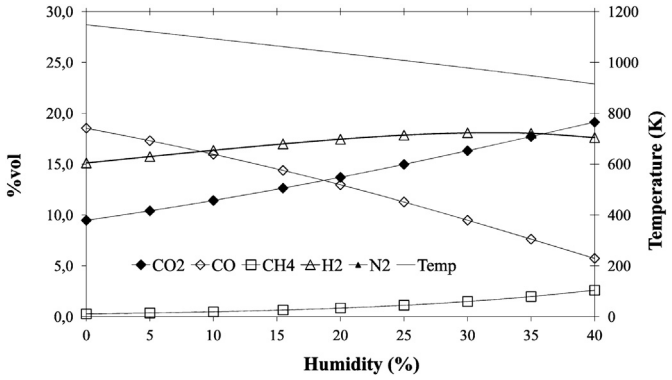

Fig. 8. Predicted producer gas composition as a function of the moisture content of the biomass ($\Phi = 2.2$).

CBP of the açaí gasification analyzed should occur at an equivalence ratio of around 2.14.

Another important operating parameter for the açaí seeds gasification is the moisture content of the biomass. Açaí seeds can have up to 70% moisture content and finding out which is reasonable moisture content for the gasification process is very important, since lowering the moisture content involves spending energy. Fig. 8 shows the predicted producer gas composition as a function of the humidity content of the biomass for an equivalence ratio of 2.2 (characteristic of maximum performance). It can be seen that an increase in the biomass humidity leads to an increase in the hydrogen content first and then to a decrease. The increase is explained by the fact that more water in the reactants favors the water shift reaction leading to an increase in hydrogen and carbon dioxide. However, more water in the reactants also leads to a decrease in the temperature (for the same equivalence ratio), which promotes the methane formation from hydrogen. After a point (around 40% moisture content), the methane reaction leads to a fast increase in the methane content and a fast decrease in the hydrogen content. It was seen from the simulations that the CO content in the producer gas decreases with the moisture content of the açaí seeds. The loss in CO of the producer gas with increasing moisture is the key aspect and determines that the heating value of the producer gas and the cold gas efficiency of the process decrease with the biomass moisture content. Additionally, fuels with moisture content above about 30% make ignition difficult [38] and are not recommended.

4. Conclusions

In the present work, 0D equilibrium simulations and experimental study assessed the gasification of açaí seeds with air, aiming at electrical power generation for small communities in Amazon region. Equivalence ratio varied between 1.5 and 4.0 for the simulations and between 1.63 and 3.14 for the experiments. Combining the experimental and numerical results, it can be concluded that gas species concentrations of CO, H_2 and CH_4 peaked when equivalence ratio was between 2.14 and 2.33, and that the cold gas efficiency, higher than 50%, was found in the same range of equivalence ratios. Additionally, the moisture content range between 30 and 40% optimizes H_2 concentration, while for CO concentrations, the most favorable moisture content range was between 0 and 25%, still keeping the H_2 concentrations higher than 15%.

References

[1] Aneel Site. www.aneel.gov.br. [accessed on January 2013].
[2] Eletrobras Site. www.eletrobras.com. [accessed on January 2013].
[3] Padilha JL. Doctoral Thesis. Universidade Federal do Pará; Brasil: 2006.
[4] Bridgwater AV. The technical and economic feasibility of biomass gasification for power generation. Birmingham: Energy Research Group, Aston University; 1995.
[5] Dornburg V, Faaij APC. Biomass Bioenergy 2001;21:91–108.
[6] Caputo AC, Palumbo M, Pelagagge PM, Scacchia F. Biomass Bioenergy 2005;28:35–51.
[7] Reed TB, Das A. Handbook of biomass downdraft gasifier engine systems. Solar technical information program. Golden, Colorado: Solar Energy Research Institute, U. S. Department of Energy; 1988.
[8] Warnecke R. Biomass Bioenergy 2000;18:489–97.
[9] Barrio M. Doctoral Thesis. The Norwegian University of Science and Technology; United States: 2002.
[10] Cruz RB, Azevedo TL, Guerra DRS. Determination of the pressure loss through a gasifier with porous fixed bed. In: Proceedings of ENCIT 2010 – 13th Brazilian congress of thermal sciences and engineering. São Paulo, São Paulo Ed. 2010.
[11] Gañan J, Al-Kassir Abdulla A, Miranda AB, Turegano J, Correia S, Cuerda EM. Renew Energy 2005;30:1759–69.
[12] González JF, Gañan J, Ramiro A, González-García CM, Encinar JM, Sábio E, et al. Fuel Process Technol 2006;87:149–55.
[13] Mamphweli NS, Meyer EL. Renew Energy 2009;34:2923–7.
[14] Yoon SJ, Son Y-I, Kim Y-K, Lee J-G. Renew Energy 2012;42:163–7.
[15] Azzone E, Morini M, Pinelli M. Renew Energy 2012;46:248–54.
[16] Vera D, de Mena B, Jurado F, Schrories G. Appl Therm Energy 2013;51:119–29.
[17] Sharma AK. Energy Convers Manag 2008;49:832–42.
[18] Puig-Arnavat M, Bruno JC, Coronas A. Renew Sustain Energy Rev 2010;14:2841–51.
[19] Zainal ZA, Ali R, Lean CH, Seetharamu KN. Energy Convers Manag 2002;42:1499–515.
[20] Altafini CR, Wander PR, Barreto R. Energy Convers Manag 2003;44:2763–77.
[21] Melgar A, Pérez JF, Laget H, Horillo A. Energy Convers Manag 2007;48:59–67.
[22] Huang HJ, Ramaswamy S. Appl Biochem Biotechnol 2009;154:193–204.
[23] Antonopoulos IS, Karagiannidis A, Gkouletsos A, Perkoulidis G. Waste Manag 2012;32:710–8.
[24] Di Blasi C. Chem Eng Sci 2000;559:2931–44.
[25] Giltrap DL, McKibbin R, Barnes GRG. Sol Energy 2003;74:85–91.
[26] Jayah TH, Aye L, Fuller RJ, Stewart DF. Biomass Bioenergy 2003;25:459–69.
[27] Babu BV, Sheth PN. Energy Convers Manag 2006;47:2602–11.
[28] Rodrigues R, Secchi AR, Marcílio NR, Godinho M. Modeling of biomass gasification applied to a combined gasifier-combustor unit: equilibrium and kinetic approaches. In: Alves RMB, do Nascimento CAO, Biscaia Jr EC, editors. Computer-aided chemical engineering, vol. 27. Elsevier; 2009. pp. 657–62.
[29] Puig-Arnavat M, Bruno JC, Coronas A. Energy Fuels 2012;36:1385–94.
[30] Jarungthammachote S, Dutta A. Energy 2007;32:1660–9.
[31] Barman NS, Ghosh S. Bioresour Technol 2012;107:505–11.
[32] Burcat A, Ruscic B. Third millennium ideal gas and condensed phase thermochemical database for combustion with updates from active thermochemical tables. Argonne, Illinois: Argonne National Laboratory; 2005.
[33] Rodrigues R. MSc Thesis. Universidade Federal do Rio Grande do Sul; Brasil: 2008.
[34] Tinaut FV, Melgar A, Giménez B, Reyes M. Fuel 2010;89:724–31.
[35] Erlich C, Fransson TH. Appl Energy 2011;88:899–908.
[36] Desrosiers R. Thermodynamics of gas-char reactions. In: Reed TB, editor. A survey of biomass gasification. Colorado: Solar Energy Research Institute; 1979.
[37] Double JM, Bridgwater AV. Sensitivity of theoretical gasifier performance to system parameters. In: Palz W, Coombs J, Hall DO, editors. Energy from biomass, proceedings of the third EC conference 1985.
[38] Mc Kendry P. Bioresour Technol 2002;83:55–63.